

Integral Equation Prediction of Reversible Coagulation in Charged Colloidal Suspensions

Victor Morales, Juan A. Anta,* and Santiago Lago

Departamento de Ciencias Ambientales, Universidad "Pablo de Olavide", Ctra. de Utrera, Km. 1, 41013 Sevilla, Spain

Received July 19, 2002. In Final Form: October 29, 2002

We exploit the accuracy of the reference hypernetted chain equation (RHNC) to study the stability of charged colloidal suspensions. To achieve this objective with confidence, we first check the performance of the RHNC integral equation by comparison with Gibbs ensemble Monte Carlo (GEMC) simulations for a simple DLVO potential. The results show that the theory describes accurately reversible coagulation into the secondary minimum for a typical intercolloidal potential. Once we have established this point, we make use of the theory to analyze the capability of the DLVO potential to describe appropriately certain experimental observations, in particular, the crossover from irreversible to reversible coagulation. In this regard we found that the inclusion of an empirical hydrophobic potential crucially affects the stability properties of the suspension and leads to an adequate prediction of the crossover diameter.

I. Introduction

The stability of colloidal suspensions has traditionally been an issue of outstanding interest among condensed-matter physicists and chemists. The celebrated Derjaguin–Landau–Verwey–Oberbeek (DLVO) theory^{1,2} has provided a very general and powerful means of predicting the stability of this kind of systems. The DLVO theory explains the well-known experimental observation that suspensions composed of charged colloidal particles become unstable (i.e. they *coagulate*) when the ionic strength of the solvent reaches a high enough (critical) value.

The DLVO theory relies on the definition of an *effective* pair interaction potential between colloids. This potential consists of two contributions: van der Waals attraction plus electrostatic repulsion, the latter being determined by the surface charge and the electrical double layer of salt ions surrounding the colloidal particles. The interplay between these two contributions leads to a potential energy function that exhibits a primary minimum at short distances, a positive potential barrier at intermediate distances, and a *secondary minimum* at large distances. As the concentration of salt increases, the electrostatic repulsion between colloids becomes more and more *screened*, and this results in a lowering of the barrier as well as of the depth of the secondary minimum. If the barrier is low enough, colloidal particles “fall” into the primary minimum and the system coagulates. This is usually referred to as *irreversible* coagulation. If the barrier is high enough to prevent irreversible coagulation, the system might still coagulate in the secondary minimum. This is a much weaker effect and is *reversible*; that is, the system can be easily redissolved by varying the conditions of the sample. Moreover, reversible coagulation depends also on the concentration (density) of colloids in such a way that coagulation can be induced if the packing fraction of colloidal particles is high enough. This fact has interesting links with biochemical processes such as those associated to the so-called *molecular crowding*.³

This work focuses on the case of coagulation in the secondary minimum. In contrast to the well studied case of coagulation in the primary minimum, the DLVO theory on its own is not capable of predicting when reversible coagulation will take place for given concentrations of salt and colloids. An extra theory is needed to solve the statistical mechanics problem posed by the DLVO interaction potential. This issue was already mentioned by Verwey and Oberbeek in their classical book² and studied theoretically by Grimson,⁴ Victor and Hansen,⁵ Kaldasch et al.,⁶ and Lai and co-workers.⁷ All these authors have employed mean-field and perturbation theories to solve the equilibrium and phase properties associated to the effect of the secondary minimum of the standard DLVO potential and related models.⁸ To our knowledge no other theoretical approaches have been applied to this issue.

In this work we employ an integral equation approach to obtain the coagulation properties of the DLVO potential. Integral equation theories^{9,10} lie among the most successful theoretical approaches in the field of the statistical mechanics description of fluids. We make use here of the reference hypernetted chain (RHNC) integral equation, which has been shown to be specially accurate in reproducing the structure and thermodynamic properties of simple liquids,^{11–13} liquid metals,¹⁴ and molecular fluids.¹⁵ The RHNC theory has also been applied successfully to obtain gas–liquid coexistence curves for a variety of

(1) Derjaguin, B. V.; Landau, L. D. *Acta Physicochim. URSS* **1941**, *14*, 633.

(2) Verwey, E. J. W.; Overbeek, J. Th. G. *Theory of the Stability of Lyophobic Colloids*; Elsevier: Amsterdam, 1948.

(3) See, for example: Shtilerman, M. D.; Ding, T. T.; Lansbury, P. T., Jr. *Biochemistry* **2002**, *41*, 3855.

(4) Grimson, M. J. *J. Chem. Soc., Faraday Trans. 2* **1983**, *79*, 817.

(5) Victor, J. M.; Hansen, J. P. *J. Chem. Soc., Faraday Trans. 2* **1985**, *81*, 43.

(6) Kaldasch, J.; Laven, J.; Stein, H. N. *Langmuir* **1996**, *12*, 6197.

(7) Lai, S. K.; Peng, W. P.; Wang, G. F. *Phys. Rev. E* **2001**, *63*, 41511.

(8) Belloni, L. *J. Phys.: Condens. Matter* **2000**, *12*, R549.

(9) Hansen, J.-P.; McDonald, I. R. *Theory of Simple Liquids*; Academic Press: London, 1986.

(10) Caccamo, C. *Phys. Rep.* **1996**, *274*, 1–105.

(11) Lado, F. *Phys. Rev. A* **1973**, *8*, 245.

(12) Lomba, E. *Mol. Phys.* **1989**, *68*, 87.

(13) Lomba, E.; Almaraz, N. G. *J. Chem. Phys.* **1994**, *100*, 8367.

(14) See, for example: Hasegawa, M.; Hoshino, K.; Watabe, M.; Young, W. H. *J. Noncryst. Solids* **1990**, *117–118*, 300. González, L. E.; Meyer, A.; Iníguez, M. P.; González, D. J.; Silbert, M. *Phys. Rev. E* **1993**, *47*, 4120. Anta, J. A.; Louis, A. A. *Phys. Rev. B* **2000**, *61*, 11400.

(15) See, for example: Fries, P. H.; Patey, G. N. *J. Chem. Phys.* **1985**, *88*, 429.

cases,^{12,16} including the (DLVO-like) hard-core Yukawa potential.¹³ A more elaborate integral equation approach has also been applied recently by some of us to describe the structure and phase behavior of a salt-free colloidal suspension.¹⁷

The objective and conclusions of this work are 2-fold. First, we pursue the utility of the integral equation approach to complement the pure DLVO theory, so that we can make reasonable predictions for the stability properties of charged colloidal systems. In this regard, the RHNC theory represents an interesting compromise between accuracy and speed of computation, especially if we are intended to evaluate coagulation properties such as the critical (reversible) coagulation concentration. To apply the RHNC results to the colloidal problem, we will make the correspondence between a simple fluid that interacts via the DLVO potential and the real system. Within this scheme, the coagulation phenomenon in the secondary minimum can be regarded as a simple gas-liquid *thermodynamic* transition where the salt concentration plays the role of an inverse temperature. In addition we will assume that coagulation in the primary minimum will not interfere with the reversible coagulation due to the energy barrier. As we will see below, this fact implies imposition of an arbitrary criterion for the RHNC *thermodynamic* results to be valid. This criterion is related to the minimum value that is allowed for the height of the barrier with respect to the average thermal energy of the particles.⁵ Also, we have checked the performance of the RHNC approach by comparing with Gibbs ensemble Monte Carlo simulations (GEMC).¹⁸ Simulations provide exact (reference) equilibrium densities for a given interaction potential (DLVO in our case). We will see that, for the cases studied, this performance is quite remarkable, especially if we compare it with the previous perturbation results.

The second objective of this work relates to the dependence of the coagulation properties on the size of the colloidal particles. In this respect, it is a general observation¹⁹ that irreversible coagulation dominates for dispersions of small particles whereas reversible coagulation is more likely for larger particles. Bearing in mind the precision exhibited by the RHNC equation to describe the secondary minimum reversible coagulation, we have made use of it to estimate quantitatively the *crossover* diameter for which transition from irreversible to reversible coagulation is expected. We have carried out this study from the *thermodynamic* or equilibrium point of view, without kinetic considerations that might be important, especially in the regime where primary and secondary minimum coagulations are likely to coexist. Nevertheless, we will see that the present approach provides a fair description of the change in the coagulation properties. In this regard we will show that, according to this model, it is necessary to go beyond pure DLVO forces to estimate accurately the transition diameter observed in the experiments. A possible explanation in terms of *hydrophobic* forces, which will modify the repulsive barrier but not the depth of the secondary minimum, is also presented in this work.

This paper is organized as follows: in section II we introduce the DLVO potential in the form that will be

used as input to the RHNC integral equation. The main features of this theory and the procedure to obtain the phase diagram are also outlined in this section. In section III we present the phase diagrams for three cases already studied in the literature and we check the RHNC results against simulation and previous perturbation theories. Direct application of the RHNC method to obtain coagulation properties and comparison with experiments are presented in section IV. Finally, our results are discussed in section V. This paper also contains an appendix that makes a short account of our method to estimate the critical point from the RHNC results.

II. Model Interaction Potential and RHNC Theory

(a) Modified DLVO Potential. According to standard DLVO theory^{2,19} the *effective* interaction between colloidal particles of diameter D immersed in a polar solvent and in the presence of added salt is made up of two contributions

$$u_{\text{DLVO}}(r) = u_A(r) + u_R(r) \quad (1)$$

where $u_A(r)$ (r being the distance between the centers of mass of the two particles) corresponds to the van der Waals attraction

$$u_A(r) = -\frac{A}{12} \left[\frac{D^2}{r^2 - D^2} + \frac{D^2}{r^2} + 2 \ln \left(1 - \frac{D^2}{r^2} \right) \right] \quad (2)$$

with A being the Hamaker's constant, and $u_R(r)$ represents the repulsive energy due to the electrical double layer of salt ions surrounding the colloids. Following Kaldasch et al.,⁶ we have used the linear superposition approximation¹⁹ to describe this electrostatic interaction. This arises from the solution of the Poisson-Boltzmann equation for spherical particles at constant *surface*, or Stern, potential ψ_0 , which yields

$$u_R(r) = \frac{16\pi\epsilon D^2}{\epsilon^2} \left[k_B T \tanh \left(\frac{e\psi_0}{4k_B T} \right) \right]^2 \frac{\exp(-\kappa(r - D))}{r} \quad (3)$$

For small values of this Stern potential, eq 3 can be approximated by²⁰

$$u_R(r) = \pi\epsilon D^2 \Psi_0^2 \frac{\exp(-\kappa(r - D))}{r} \quad (4)$$

where ϵ is the dielectric constant of the solvent and κ is the inverse Debye length. The inverse Debye length is directly related to the valence z_i and density ρ_i of all *charged* species i present in the sample

$$\kappa = \sqrt{\frac{e^2}{\epsilon k_B T} \sum_i \rho_i z_i^2} \quad (5)$$

with e being the elementary charge and k_B the Boltzmann constant. At this point it is important to note that the resulting effective potential is, as a matter of fact, *density-dependent*; that is, it depends on the concentration of

(16) See, for example: Caccamo, C.; Giunta, G.; Malescio, G. *Mol. Phys.* **1995**, *84*, 125. Anta, J. A.; Lomba, E.; Alvarez, M.; Lombardero, M.; Martín, C. *J. Phys. Chem. B* **1995**, *101*, 1451.

(17) Anta, J. A.; Lago, S. *J. Chem. Phys.* **2002**, *116*, 10514.

(18) Panagiotopoulos, A. Z. *Mol. Phys.* **1987**, *61*, 247.

(19) Russel, W. B.; Saville, D. A.; Schowalter, W. R. *Colloidal Dispersions*; Cambridge University Press: 1989.

(20) This is a linearized version of the general DLVO potential (see, e.g., ref 19, eq 4.10.13) which is assumed to be valid for surface potentials smaller than 25 mV. Nevertheless, for the highest of the surface potentials actually used in our work, that is, 29 mV, the potential barrier in the nonlinear potential is 7.9% lower than that in the linearized potential and the secondary minimum is only 1.4% deeper than that in the linearized potential. This should not affect significantly the coagulation properties in the regime considered in this work.

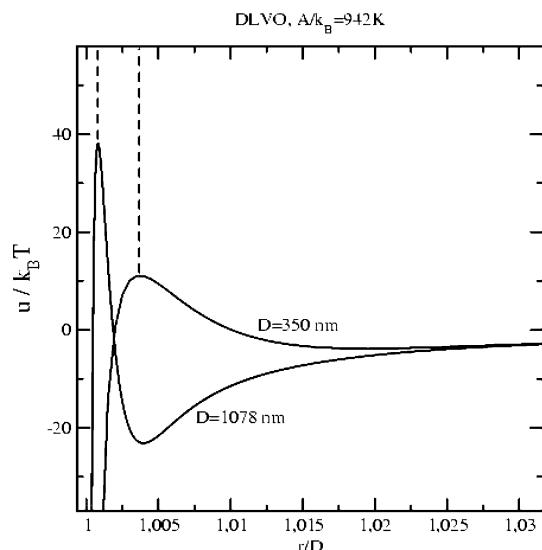


Figure 1. DLVO interaction potentials for colloidal dispersions considered in this work. The Hamaker constant is $A = 1.3 \times 10^{-20} \text{ J}$ ($A/k_B = 942 \text{ K}$) in both cases whereas the Stern potentials are 23 and 28 mV for the small and the large diameter, respectively. The inverse Debye lengths used to compute the potentials are $\kappa D = 214.1$ (350 nm) and $\kappa D = 1011.7$ (1078 nm), corresponding to experimental critical coagulation concentrations at these conditions.³² The dashed lines mark the points where the DLVO is replaced by a hard-core repulsive interaction (see text).

colloidal particles. This is because the colloids and the counterions (produced by ionization of the colloids) contribute to the total ionic strength.⁸ The main consequence of this is that $u_R(r)$ should be recalculated when the concentration of colloidal particles is varied. Nevertheless, it is easy to show that for concentrations of salt like those normally utilized in experiments ($>0.01 \text{ M}$) the contribution of counterions is negligible and the electrostatic interaction between colloidal particles is only controlled by the screening due to the salt ions. Thus, for the experimental regime that we are interested in (high and moderate salt concentrations), the DLVO potential is, effectively, *density-independent*.²¹ Also, we should bear in mind that all thermodynamic properties that we will obtain for this potential will be *osmotic*; that is, they correspond to the system of colloids on its own and are defined with respect to a reservoir containing salt ions only.²¹ In the osmotic scenario the inverse Debye length is an external parameter that simply tunes the range of the interaction. Incidentally, the word *osmolarity* is the usual term in medical journals²² to describe exactly the same effect.

The DLVO potential defined by eqs 1, 2, and 4 is plotted in Figure 1 for some values of the diameter and the inverse Debye length. As mentioned above, one of the main features of this potential is the attractive primary minimum at short distances. This is a consequence of the fact that the attractive van der Waals contribution always

wins when the two colloidal spheres are in contact (note that $u_A(r) \rightarrow -\infty$ as $r \rightarrow D$ whereas $u_R(r)$ remains finite). As the primary minimum is infinitely deep and the positive potential barrier is always finite, the colloidal system as described by the DLVO potential is *thermodynamically unstable*. In other words, at equilibrium the stable state is the *coagulated* state. Only if the positive potential barrier is high enough with respect to the average thermal energy of the particles can coagulation in the primary minimum be slow enough to stabilize effectively the system. Thus, the system becomes *kinetically stable* although thermodynamically unstable. Nevertheless, thermodynamics is not concerned about kinetics, and if we apply a purely thermodynamic or *equilibrium* method such as the RHNC theory, we will always be predicting irreversible coagulation even if this is not the case (in kinetic and practical terms). To surmount this problem, Victor and Hansen⁵ ignored completely the primary minimum by replacing the short-range behavior of the DLVO potential by a purely repulsive interaction. Following this strategy, we take a modified DLVO potential defined by

$$u(r) = \begin{cases} \infty & r < r_{\max} \\ u_{\text{DLVO}}(r) & r > r_{\max} \end{cases} \quad (6)$$

where r_{\max} corresponds to the position of the positive energy barrier (see Figure 1). Obviously this scheme for replacing a kinetically stable system by a thermodynamically stable one is only valid if the potential barrier is very high in comparison with the average thermal energy of the colloidal particles, say⁵ $u_{\text{DLVO}}(r_{\max}) > 10k_B T$ or⁷ $u_{\text{DLVO}}(r_{\max}) > 15k_B T$. In this work we have taken the first of these values as a convenient choice.²³ Nevertheless, we should bear in mind that the results presented here should be taken with some reserve when the energy barrier approaches this limit. For smaller values of the height of the energy barrier, we should assume that there is a somehow indefinite region where irreversible and reversible coagulation will coexist.

(b) RHNC Theory of Simple Liquids. In its simplest form, the RHNC theory applies to a collection of N particles that interact via a pairwise additive density-independent potential $u(r)$. Under these prescriptions the microscopic structure and thermodynamics of the system are completely determined by the radial distribution function $g(r)$. In the canonical ensemble, that is, for number of particles N , volume V , and T fixed, this is defined by⁹

$$g(r) = \frac{V^2 \int d\mathbf{r}^{N-2} \exp[-\beta \sum_{i < j} u(r_{ij})]}{\int d\mathbf{r}^N \exp[-\beta \sum_{i < j} u(r_{ij})]} \quad (7)$$

with $\beta = 1/k_B T$.

The RHNC theory provides an approximate but highly accurate way to obtain $g(r)$. Starting from a functional Taylor expansion of the excess free energy in terms of density derivatives,^{9,24} it is possible to express $g(r)$ in the form

(21) More rigorously, we can consider our system as a collection of colloidal particles in the presence of a reservoir of salt of constant chemical potential.⁸ This is equivalent to assuming that we are working in a semi-grand-canonical ensemble where the number of colloids, the temperature, and the volume are kept constant but where the number of salt ions is allowed to fluctuate. In this way, any change in composition in the system is counterbalanced by osmotic equilibrium so that the inverse Debye length remains constant. Since all statistical ensembles are equivalent in the thermodynamic limit, this provides validity to our thermodynamic calculations of osmotic properties with the effective colloid–colloid DLVO potential.

(22) Fontaine, O. *Lancet* **1995**, 345, 282.

(23) Consider that for $u_{\text{DLVO}}(r_{\max}) > 10k_B T$, and according to the Arrhenius equation, irreversible coagulation is of the order of 22000 times slower than that in the system where the energy barrier vanishes.

(24) See, for example: Xu, H.; Hansen, J.-P. *Phys. Rev. E* **1998**, 57, 211. Anta, J. A.; Louis, A. A. *Phys. Rev. B* **2000**, 61, 11400.

$$g(r) = \exp[-\beta u(r) + h(r) - c(r) - B(r)] \quad (8)$$

where $h(r) = g(r) - 1$ and $c(r)$, the *direct correlation function*, can be defined via the Ornstein–Zernike equation^{9,10}

$$h(r) = c(r) + \rho \int c(|\mathbf{r} - \mathbf{r}'|) h(r') d\mathbf{r}' \quad (9)$$

where $\rho (=N/V)$ is the number density of particles and $B(r)$ is the *bridge function*, which is related to the higher-than-two density functional derivatives of the excess free energy. If we assume $B(r) = 0$, eqs 8 and 9 constitute a closed relation that determines $g(r)$ for given temperature and density. This is the HNC approximation. Within the RHNC scheme, the bridge function is not neglected but is assumed to be equal to the bridge function of a suitable reference potential.²⁵ Customarily this reference potential is taken to be the hard-sphere potential, which is defined by a single parameter, the hard-sphere diameter D . Thus, in the RHNC approximation²⁶

$$B(r) \approx B^0(r, D) \quad (10)$$

where $B^0(r, D)$ is the bridge function of a fluid of hard spheres of diameter D . Now eqs 8–10 define the $g(r)$ for given temperature and density, provided we have a means to specify the optimum hard-sphere diameter D . Lado, Foiles, and Ashcroft²⁷ applied a criterion of minimization of the total free energy of the system to obtain D . They found the following optimization condition for D

$$\int [g(r) - g^0(r, D)] D \frac{\partial B^0(r, D)}{\partial D} d\mathbf{r} = 0 \quad (11)$$

where $g^0(r, D)$ is the radial distribution function of the hard-sphere fluid of diameter D . In this work we have used the parametrical expressions of Verlet and Weis²⁸ and Labík and Malyjevsky²⁹ for the radial distribution function and bridge function of the hard-sphere fluid, respectively.

As we are mainly interested in the computation of the phase diagram, the keystone of the present formalism is the evaluation of the free energy. Lado, Foiles, and Ashcroft²⁷ found the following approximate expression for the excess free energy within the RHNC approximation

$$\begin{aligned} \frac{F^{\text{ex}}}{Nk_B T} = & \frac{1}{2}\rho \left(\frac{1}{\rho \chi_T k_B T} - 1 \right) + \\ & 2\pi\rho \int_0^\infty r^2 g^0(r, D) B^0(r, D) dr - \\ & \frac{1}{4\pi^2\rho} \int_0^\infty \left\{ \rho^2 \tilde{h}(k) \left(\tilde{c}(k) - \frac{1}{2} \tilde{h}(k) \right) + \right. \\ & \left. \ln(1 - \rho \tilde{h}(k)) - \rho \tilde{h}(k) \right\} k^2 dk \quad (12) \end{aligned}$$

where χ_T is the isothermal compressibility and $h(k)$ and $c(k)$ are sine Fourier transformations of the functions $h(r)$ and $c(r)$, respectively.

(c) Numerical Details and Evaluation of the Phase Diagram. The RHNC integral equation is solved numerically on a grid of 4096 points with a grid size of $0.005D$ in real space. The method of Ng³⁰ combined with Broyles'

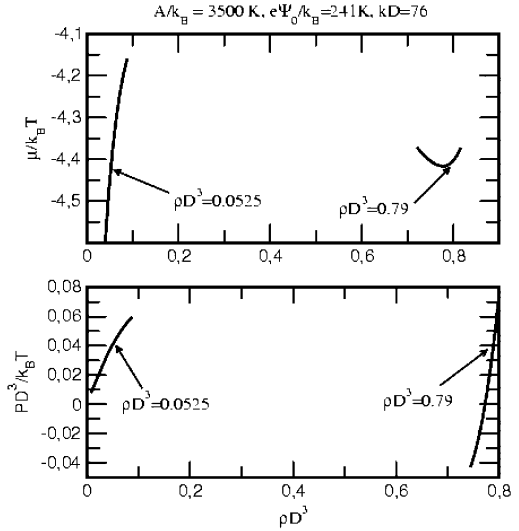


Figure 2. Chemical potential and pressure as computed by the RHNC equation for the modified DLVO interaction (see text). The parameters that define the potential are shown in the upper panel. The arrows mark the densities for which phase equilibrium (equal pressures and chemical potentials) is found in this case.

strategy³¹ to mix conveniently successive estimates of the correlation functions is employed to enhance the convergence in the numerical solution. To obtain the phase diagram, we proceed as follows: we solve consecutively the integral equation for successive colloidal concentrations ρ at constant temperature and κ , starting from the limit of zero colloidal concentration. For each ρ we then evaluate and store the osmotic pressure and chemical potential by means of

$$\beta P = \rho - \frac{2}{3}\pi\rho^2 \int_0^\infty r^3 \frac{d\beta u(r)}{dr} g(r) dr \quad (13)$$

$$\beta\mu = \log \rho + \beta F^{\text{ex}}/N + \beta P/\rho + f(T) \quad (14)$$

where $f(T)$ contains the temperature-dependent terms of the ideal gas free energy and $\beta F^{\text{ex}}/N$ is given by eq 12.

We start from a small enough value for κ . If the RHNC finds a solution for all concentrations, this means that the critical κ lies at higher values. We then increase the value of κ and run the corresponding “isotherm” until we bump into a nonsolution boundary.¹² This marks approximately the locus of the “gas” or low-concentration side of the coexistence line. We then move to the “liquid” or high-concentration side and run the corresponding “isotherm” for the same κ until no-solution. To run the “liquid” isotherm, we need to start from a previous high-density solution, which can be obtained from previous solutions at *subcritical* κ values. Once we have the “gas” and “liquid” isotherms for the same κ , the coexisting densities are then obtained by solving the phase equilibrium conditions (see Figure 2)

$$P_{\text{gas}} = P_{\text{liquid}}$$

$$\mu_{\text{gas}} = \mu_{\text{liquid}} \quad (15)$$

This process is repeated for several values of the inverse Debye length κ . As it is not possible to get convergent solutions of the RHNC equation in the vicinity of the critical point, we estimate the location of the critical point

(25) Rosenfeld, Y.; Ashcroft, N. W. *Phys. Rev. A* **1979**, *20*, 1208.

(26) Lado, F. *Phys. Rev. A* **1973**, *8*, 245.

(27) Lado, F.; Foiles, S. M.; Ashcroft, N. W. *Phys. Rev. A* **1983**, *28*, 2374.

(28) Verlet, L.; Weis, J. J. *Phys. Rev. A* **1972**, *5*, 939.

(29) Labík, S.; Malyjevsky, A. *Mol. Phys.* **1989**, *67*, 431.

(30) Ng, K. *J. Chem. Phys.* **1974**, *61*, 2680.

(31) Broyles, A. A. *J. Chem. Phys.* **1960**, *33*, 2680.

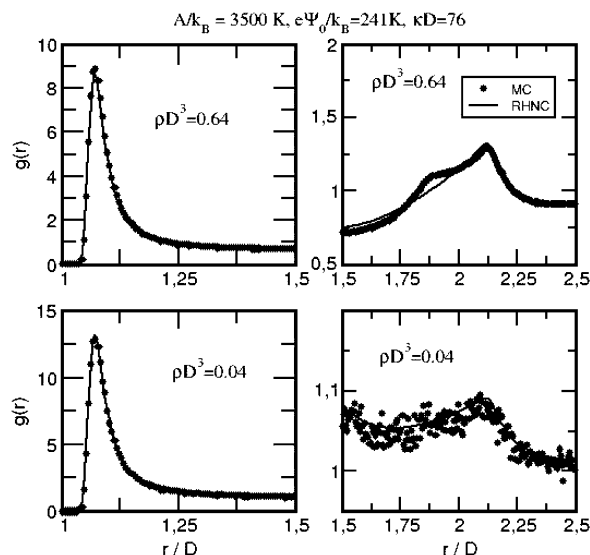


Figure 3. Radial distribution functions for a colloidal dispersion modeled by the modified DLVO potential with the parameters shown at the top. MC refers to data extracted from our GEMC simulations, which also provide results for the structure in both the “gas” and “liquid” phase.

(ρ_C , κ_C) by means of a suitable extrapolation of the RHNC equilibrium densities (see the Appendix).

III. “Gas–Liquid” Equilibrium for the Modified DLVO Potential

In this section we present RHNC results for the phase behavior of the modified DLVO potential introduced above and compare them with GEMC simulations and previous perturbation theories.^{6,7} The aim of this is to check the exactitude of the theory regardless of the accuracy of the potential. All results presented here correspond to room temperature and $\epsilon = 78.5$, that is, standard conditions corresponding to an aqueous solvent at room temperature. GEMC simulations¹⁸ were performed with $N = 1000$ particles distributed initially in two boxes with equal initial density $\rho D^3 = 0.4$ (500 particles in a box of volume $1250 D^3$). Runs consisted of 50 000–150 000 equilibration steps and 50 000–150 000 production steps, each step comprising N attempts to move a particle, one attempt to change the volume and $2000N$ attempts to interchange particles between the boxes. With these parameters the GEMC calculations showed phase separation for inverse Debye lengths above a certain critical value, κ_C . Once phase separation is reached, the simulations provide equilibrium coexisting densities with equal values (within the statistical uncertainty of the simulation) of the pressure and chemical potential. We should point out that the GEMC simulations for the modified DLVO potential here studied correspond, as a matter of fact, to a *semi-grand canonical Gibbs* ensemble. In this situation the two boxes containing colloidal particles are assumed to be in contact with a “thermal bath” of salt particles that keeps the concentration of ions (and hence κ) constant in both phases. This corresponds exactly to the same situation that was assumed when we introduced the RHNC formalism described in the previous section (a DLVO potential with constant κ) and tries to represent the experimental situation in which we have colloidal particles moving in a solvent with constant concentration of salt.

We have also extracted from the simulation the radial distribution functions for colloids. Comparison with the RHNC predictions for the “gas” and “liquid” phases is shown in Figure 3. This plot illustrates the remarkable

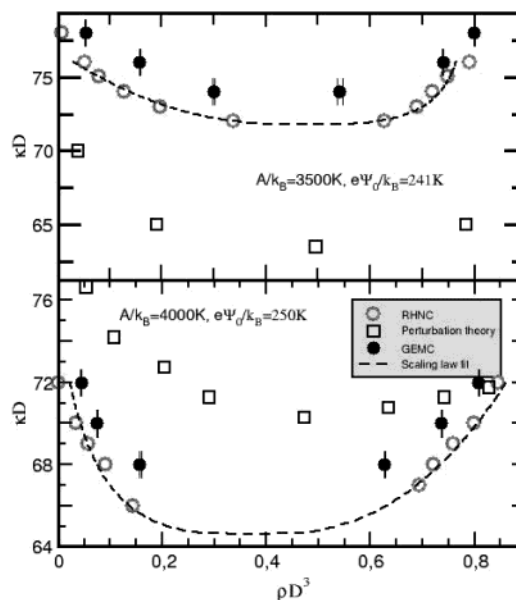


Figure 4. “Gas–liquid” phase diagrams showing secondary minimum coagulation for colloidal dispersions modeled via the modified DLVO potential. Perturbation theory results are taken from ref 6. The dashed lines stand for a scaling law fit of the RHNC equilibrium densities (see Appendix).

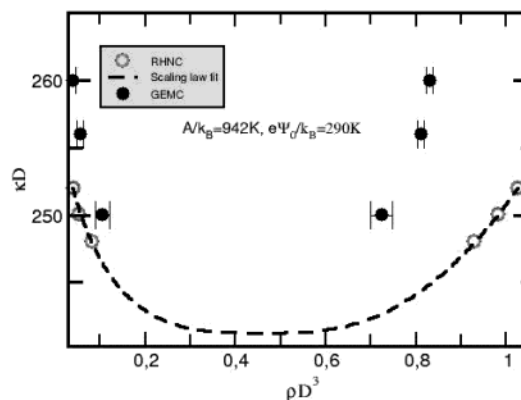


Figure 5. Same as Figure 4 but for colloidal dispersions with parameters as shown. The dashed line has the same meaning as in Figure 4. The results from perturbation theory⁷ lie far outside of the figure.

accuracy of the integral equation to describe the pair structure, a well-known fact as regards the RHNC theory.¹⁰ This accuracy in the description of the pair structure somehow explains the good performance exhibited by the theory in the estimation of the phase equilibrium properties. The results for these properties are presented in Figures 4 and 5. The first thing to note is that, for all cases studied, RHNC “gas–liquid” coexistence lines lie closer to the “exact” GEMC results than the perturbation theory predictions of refs 6 and 7. This is specially striking in the case considered in Figure 5, where the RHNC and GEMC critical κ (around $240 D^{-1}$) disagrees considerably with the value reported by Lai and co-workers⁷ for the same DLVO parameters: $393.7 D^{-1}$. This discrepancy cannot be due to the dependency of the potential on the colloidal density, as the alternative model that takes into account this effect leads essentially to the same results.⁸

Leaving apart the discrepancy between our present results and previous approaches, the comparison between RHNC theory and simulation shows that the integral equation always *underestimates* the critical κ . This could be expected in consideration of the performance of the

RHNC theory when describing gas–liquid equilibrium (RHNC results for simple and molecular fluids always *overestimate* the critical temperature^{12,15}). Also, for the case studied in Figure 5, the “liquid” RHNC coexisting densities exhibit a large error when compared with the “exact” GEMC values, although this mismatch does not seem to lead to a large displacement of the critical point. Despite these disagreements, the RHNC method utilized here proves to be quite accurate to describe phase separation for the modified DLVO potential. As this modified interaction contains the secondary-minimum features of the DLVO potential, the present procedure turns out to be a useful tool to describe reversible coagulation. Moreover, it should be taken into account that the RHNC procedure is a much more rapid way of obtaining the phase diagram than using simulation. Just for comparison, performing a GEMC simulation for a given κ value takes around 300 h of CPU time in a 1.50 GHz PC, whereas evaluating the coexisting densities via solution of the RHNC equation is a matter of a few minutes.

IV. Reversible versus Irreversible Coagulation. Role of Hydrophobic Forces

Once we have established the reliability of the RHNC theory to obtain equilibrium properties for the DLVO model, we can turn to make use of it in order to draw conclusions concerning the stability of real colloidal suspensions. As mentioned in the Introduction, colloidal suspensions composed of small particles are likely to coagulate irreversibly upon salt addition whereas large colloidal particles tend to coagulate reversibly under the same conditions.¹⁹ This is a direct consequence of the dependence of the repulsive part of the DLVO potential on the colloidal diameter (see eq 3), which makes the repulsive barrier higher for larger sizes. As the depth of the secondary minimum also increases with size, both effects combined lead to the preeminence of reversible coagulation for large colloidal particles. In connection with this issue, Lai and co-workers⁷ studied very thoroughly the transition between irreversible and reversible coagulation and compared their results with experimental observations.³² Their approach was based on a comparison of the relative values of the attractive and repulsive parts of the colloid–colloid potential. Nevertheless, the quantitative prediction of reversible coagulation requires in their formalism the use of perturbation theory in order to obtain the “gas–liquid” phase diagram.

In the previous section we have tried to show that perturbation theory does not seem to be accurate enough in predicting the critical inverse Debye length for coagulation in the secondary minimum. This affects the conclusions of ref 7 concerning the regions of dominance of reversible and irreversible coagulation. To clarify this point, we have calculated by means of the RHNC method the phase diagrams (and from them the κ values) of the same systems studied experimentally. The results for the κ values of reversible (secondary minimum) coagulation are plotted in Figure 6 as a function of colloidal size. The experimental values³² of both irreversible and reversible coagulation for a suspension of “soap-free” polystyrene latex particles are also included in the figure. At this point it is necessary to mention that the “crossover” diameter that differentiates between both types of coagulation seems to lie, according to the experiments, around 700–800 nm. The κ values which make the repulsive barrier of the DLVO potential vanish are plotted in the same figure as well.

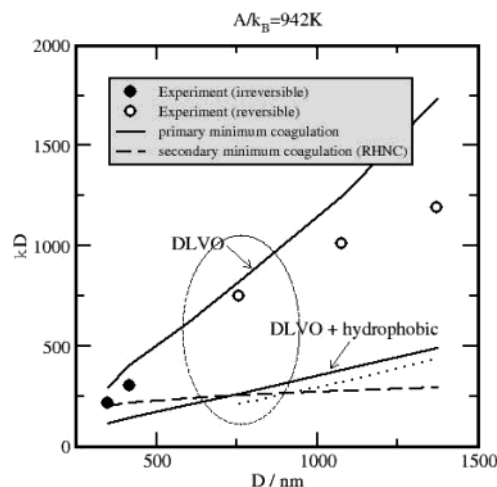


Figure 6. Critical coagulation κ values for dispersions of polystyrene latex particles of different diameters as reported in the experimental work of Kotera and co-workers.³² An explicit distinction between irreversible and reversible coagulation is made when plotting these points. In all cases the Hamaker constant is $A = 1.3 \times 10^{-20}$ J ($A/k_B = 942$ K) and the Stern potentials are 23, 25, 27, 28, and 29 mV for the diameters 350, 416, 758, 1078, and 1374 nm, respectively (see Figure 1 for the actual shape of the DLVO potential for two of these cases). The dashed line represents the predictions of the RHNC theory for coagulation in the secondary minimum using the corresponding modified DLVO potentials. The effect of adding an empirical hydrophobic interaction to the DLVO potential (see text) is also shown in the figure. Note that the solid lines correspond to primary minimum coagulation values only. These values were obtained using the criterion of setting the repulsive potential value to zero.¹⁹ If the criterion is that the barrier reaches a value of $10k_B T$, then we get the dotted line (here plotted for DLVO plus hydrophobic forces only). The ellipse indicates the region in which transition from irreversible to reversible coagulation is observed.

Examination of Figure 6 reveals that, according to the approach put forward in this work, secondary minimum coagulation always lies at *lower* salt concentrations than primary minimum coagulation. Only at small colloidal sizes is the “distance” between both types of coagulation reduced. This might explain, as found in ref 7, the transition from irreversible to reversible coagulation. Nevertheless, if the RHNC results are to be trusted, reversible coagulation would occur prior to primary coagulation for all cases as we add salt to the system. In fact, for the smallest diameter studied (350 nm), the DLVO potential still exhibits a quite substantial potential barrier (of the order of $11k_B T$) at the experimental critical coagulation concentration (see Figure 1). All these considerations suggest that there might be in the experiments extra forces that are not of DLVO origin. These forces should be necessarily attractive so that the height of the potential barrier is reduced (and so the primary minimum critical coagulation κ) and/or the depth of the secondary minimum is augmented (and hence the secondary minimum coagulation κ value is increased).

In connection to this point, we have explored the effect of non-DLVO forces of the hydrophobic type. The effect of hydrophobic interactions on the stability of latex suspensions has already been mentioned in the literature.³³ These forces are always present whenever we have organic colloidal particles dissolved in water and produce a net *attractive* contribution to the total colloidal potential due to the unfavorable interaction between the hydrophobic surface and the water molecules.^{34,35} Experimental mea-

(32) Kotera, A.; Furosawa, K.; Kubo, K. *Kolloid Z. Polym.* **1970**, 240, 837.

(33) Kostansek, E. C. *Trends Polym. Sci.* **1996**, 4, 383.

surements of the hydrophobic forces between flat surfaces in water lead to the empirical expression³⁴

$$E_H = -2\gamma \exp(-H/\lambda) \quad (16)$$

where E_H is the energy per unit surface as a function of the distance H between the surfaces, and γ and λ are empirical parameters whose values range between 10 and 50 mJ/m² and between 1 and 2 nm, respectively. To obtain the hydrophobic contribution to the interaction between spherical colloidal particles, we apply the Derjaguin approximation^{1,34} to eq 16 to arrive at

$$u_H(r) = -\pi D\gamma\lambda \exp(-(r - D)/\lambda) \quad (17)$$

where r is the center-to-center distance between colloidal particles.

The hydrophobic contribution of eq 17 is actually very short-ranged (recall that $\lambda = 1-2$ nm) and affects only the region of the DLVO potential where the barrier appears (see Figure 1). As hydrophobic forces are attractive, the final effect is to reduce the height of the barrier without modifying the depth of the secondary minimum. This results in a reduction of the κ values of primary minimum coagulation. In Figure 6 we have included these values for the case in which $\gamma = 50$ mJ/m² and $\lambda = 1$ nm. We have chosen these values because in this case the line corresponding to primary minimum coagulation crosses the secondary minimum line exactly in the region where the transition from irreversible to reversible coagulation is detected in the experiments. This provides a simple *thermodynamic* explanation for the coagulation behavior found experimentally. Nevertheless, this conclusion should be taken with reserve, due to the large disagreement between experimental and RHNC critical coagulation concentrations. As discussed below, this disagreement evidences that either the intercolloidal potential is not known accurately enough or kinetic effects are much more important than expected.

V. Discussion and Conclusions

Two main conclusions can be extracted from the results presented in this paper. On one hand the RHNC integral equation is a rapid and accurate theoretical tool to test interaction potentials in colloidal suspensions. We have seen, by comparing with simulation, that it produces accurate values of the "gas-liquid" coexistence curves of a modified DLVO potential which represents the interaction between particles in *kinetically* stabilized colloidal suspensions. The predicted critical values of the inverse Debye length lie, at least for the cases here considered, close to the "exact" values extracted from GEMC simulations. At the same time, the coexistence curves here obtained disagree considerably with respect to the perturbation theory results already reported in the bibliography. On the basis of the agreement between RHNC theory and simulation, we assume that our theory is reliable and that it can be used with confidence to predict reversible coagulation properties in this kind of systems. In addition, the integral equation is rapid from the computational point of view and this permits us to obtain quick conclusions for a *given* model potential of the colloidal interaction.

(34) Israelachvili, J. N. *Intermolecular and surface forces*; Academic Press: 1992.

(35) Southall, N. T.; Dill, K. A.; Haymet, D. J. *J. Phys. Chem. B* **2002**, *106*, 521.

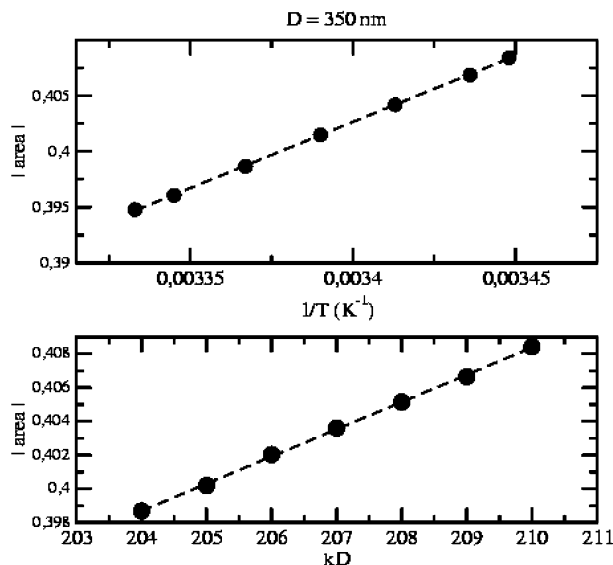


Figure 7. Absolute values for the area bounded by the modified DLVO potential with respect to the x -axis versus the inverse temperature (upper panel) and the inverse Debye length (lower panel). The dashed lines are linear fits of the values shown.

On the other hand, direct comparison between theory and experiment leads to intriguing results. First of all, the RHNC κ values for reversible coagulation differ considerably from the experimental ones. Second, the locations of the primary and secondary minimum coagulation boundaries imply that reversible coagulation will always occur at lower salt concentrations than those for irreversible coagulation for the range of sizes here considered. According to the present RHNC results, the transition between irreversible and reversible coagulation would be produced at colloidal diameters much smaller than those observed experimentally. We have seen that the addition of a hydrophobic interaction with realistic empirical parameters makes it possible that the irreversible-reversible transition occurs at the right diameter. Nevertheless, the experimental values for the critical κ still lie far from the theoretical predictions, especially for large particles. If we assume that the RHNC predictions for the DLVO potential are accurate enough (as the agreement with the GEMC "exact" values seems to imply), we should consider that still there are effects which are not well accounted for in the DLVO interaction here considered.

Acknowledgment. This work has been supported by the Spanish Dirección General de Investigación Científica y Técnica under grant BQU2001-3615-C02-01 and Instituto de Salud Carlos III under Grant 01/1664. We also thank Dr. Romero-Enrique for interesting comments.

Appendix: Estimation of the Critical Point from RHNC Results

It is a well-known fact the RHNC theory fails to yield results in the vicinity of the critical point.¹² Nevertheless, by using suitable *scaling laws*, it is possible to extrapolate the coexistence lines obtained from the application of the equilibrium conditions and locate the position of the critical point. Thus, we can estimate the critical parameter by fitting the gas and liquid equilibrium densities to the equations

$$\rho_l - \rho_g = A(T - T_c)^\beta$$

$$\frac{\rho_l + \rho_g}{2} = \rho_C + B(T - T_C) \quad (\text{A-1})$$

where ρ_C and T_C are the critical density and temperature, respectively, A and B are numerical constants, and β is the critical exponent.³⁶ The use of an Ising-like exponent of $\beta = 1/3$ proved to be rather accurate in previous RHNC studies.^{12,13,16} The problem posed in the context of this work is that we do not have equilibrium densities in terms of *true* temperatures but in terms of inverse Debye lengths. Therefore, it is necessary to extend the expressions of eq A-1 in the sense that they describe a coexistence curve where the two entries are κ values and densities instead of temperatures and densities. We could convert eqs A-1 easily if we had an expression that relates the inverse Debye length to the temperature. To do this, we have examined how the DLVO potential *scales* with κ and compared the resulting behavior with the same scaling but with respect to the temperature. Since the gas–liquid transition is controlled by the attractive part of the potential, we have chosen the area bounded by the DLVO

potential with respect to the x -axis as an appropriate parameter to measure the scaling. Following this line of reasoning in Figure 7, we have plotted these area values as a function of inverse temperature and κ . In both cases the DLVO potential scales *linearly* with the chosen parameter. This means that k tunes the *attraction* the same way as $1/T$ does. Therefore, it is legitimate to replace $1/T$ by k in the laws that describe how the system approaches the critical point. According to this argument, we convert eqs A-1 into

$$\begin{aligned} \rho_l - \rho_g &= A' \left(\frac{\kappa - \kappa_C}{\kappa} \right)^\beta \\ \frac{\rho_l + \rho_g}{2} &= \rho_C + B' \left(\frac{\kappa - \kappa_C}{\kappa} \right) \end{aligned} \quad (\text{A-2})$$

where A' and B' are numerical constants distinct, in principle, from their counterparts in eq A-1. Fitting the RHNC equilibrium densities to these formulas with a critical exponent of $\beta = 1/3$ provides a very good match of the coexistence curve and hence a reliable estimation of the critical density and κ_C .

(36) Binney, J. J.; et al. *The Theory of Critical Phenomena*; Clarendon Press: Oxford, 1999.